Yonsei Medical Journal
Vol. 43, No. 2, pp. 211 - 222, 2002

Original Article

Significance of ^{99m}Tc-ECD SPECT in Acute and Subacute Ischemic Stroke: Comparison with MR Images Including Diffusion and Perfusion Weighted Images

Hyun-Sook Kim[1], Dong-Ik Kim[2], Jong Doo Lee[3], Eun-Kee Jeong[2], Tae-Sub Chung[2], Pyeong-Ho Yoon[2], Seung-Koo Lee[2], Eun-Ju Kim[4], Yong Kyu Yoon[1], Bum-Chun Suh[5], and Byung-In Lee[5]

[1]Department of Diagnostic Radiology, Eulji University School of Medicine, Taejon, Korea;
Departments of [2]Diagnostic Radiology, [3]Division of Nuclear Medicine, [4]Medicine, [5]Neurology, Yonsei University Medical College, Seoul, Korea.

^{99m}Tc-ECD SPECT is valuable for the evaluation of cell viability and function. The purpose of the present study was to evaluate the significance of ^{99m}Tc-ECD brain SPECT in ischemic stroke. We compared ^{99m}Tc-ECD brain SPECT with perfusion and diffusion weighted images (PWI, DWI). Ten patients with acute and early subacute ischemic stroke were included in this prospective study. T2-weighted images (T2WI), DWI, PWI and ^{99m}Tc-ECD SPECT were obtained during both the acute/early subacute and late subacute stages. In the case of PWI, time to peak (TTP) and regional cerebral blood volume (rCBV) maps were obtained. The rCBV map and ^{99m}Tc-ECD SPECT images were compared in 8 lesions using ΔAI. The asymmetry index (AI) was calculated as (Ci - Cc) $\times$ 200 / (Ci + Cc); where Ci is the mean number of pixel counts of an ipsilateral lesion and Cc is the mean number of pixel counts of the normal contralateral hemisphere. ΔAI was defined as $AI_{acute} - AI_{subacute}$ in the ischemic core and periphery. PWI and ^{99m}Tc-ECD SPECT detected new lesions of the hyperacute stage or of evolving stroke more accurately than T2WI and DWI. ^{99m}Tc-ECD SPECT was able to localize the infarct core and peri-infarct ischemia in all lesions in both the acute and the subacute stages. ΔAI was higher in the rCBV map than in the ^{99m}Tc-ECD SPECT images in the ischemic core ($p = 0.063$) and in the periphery ($p = 0.091$). In the ^{99m}Tc-ECD SPECT images, ΔAI was higher in the ischemic core than in the periphery ($p = 0.028$). During the subacute stage, ^{99m}Tc-ECD SPECT detected all the lesions without the pseudonormalization seen in the MR images of 5/11 lesions. Based on this study, ^{99m}Tc-ECD SPECT is comparable to PWI in terms of its ability to detect acute stroke and is more useful than PWI in the case of subacute infarction.

Key Words: Cerebral infarction, technetium-99m-ethyl cysteinate dimer, single photon emission computed tomography, magnetic resonance imaging, diffusion, perfusion

Received July 26, 2001
Accepted January 24, 2002

Reprint address: requests to Dr. Dong-Ik Kim, Department of Diagnostic Radiology, Yonsei University College of Medicine, C.P.O. Box 8044, Seoul 120-752, Korea. Tel: 82-2-361-5837, Fax: 82-2-393-3035, E-mail: dikim@yumc.yonsei.ac.kr

INTRODUCTION

Single photon emission computed tomography (SPECT), using radiolabeled blood flow tracers such as HMPAO, ECD and IMP, is known to be useful for detecting acute ischemic stroke by demonstrating hypoperfusion earlier than conventional MR images. However, the spatial resolution of brain SPECT is less than that of MR images, and "hyperfixation" of the ^{99m}Tc-HMPAO within the area of luxury perfusion limits the precise evaluation of its viability during the subacute stage.[1] Since ^{99m}Tc-ECD was introduced by Cheeseman et al.,[2] ^{99m}Tc-ECD brain SPECT has become a good marker of regional cerebral blood flow (rCBF) and has proven to be useful for the evaluation of cellular viability even in cases of luxury perfusion.[2-5]

In the case of MR images, conventional T1-weighted images (T1WI), T2-weighted images (T2WI) and fast spin-echo (FSE) T2 images depict acute ischemic areas with good anatomic resolution, but these techniques are limited in terms of their abilities to detect lesions during the 24 hours following an ischemic attack.[6,7] Perfusion-weighted images (PWI) including, cerebral blood

volume (CBV), mean transit time (MTT) and CBF images provide information which supplements those that obtained from conventional MR imaging of the regional microcirculation. In particular, PWI combined with diffusion-weighted images (DWI) allows regional assessment of the tissue at risk by providing a PWI/DWI mismatch in the case of acute ischemic stroke,[8-12] which is valuable for selecting those patients that require intensive thrombolytic and neuroprotective therapies.

The purpose of the present study was to compare ^{99m}Tc-ECD brain SPECT with MR images, including PWI and DWI, and to evaluate the role of ^{99m}Tc-ECD SPECT in stroke patients.

MATERIALS AND METHODS

Subjects

Ten patients (7 males and 3 females; mean age, 59 years; range, 28 to 75 years) with acute (6 - 24 hr) and early subacute (24 - 72 hr) stage of MCA territory infarction were included in this prospective study (Table 1). Patients with abrupt onset of hemiplegia and the evidence of recent MCA infarction on DWI were consecutively selected for the study. Patients showing involvement of more than two-thirds of the hemisphere or hemorrhagic transformation in the initial MRI or recent infarction of the vertebrobasilar system were excluded from the study. The mechanisms of the strokes were classified using 'Trial of ORG 10172 in Acute Stroke Treatment' (TOAST) criteria.[13] Patients received conservative management. This study was approved by the institutional review board and informed consent was obtained from patients or their authorized representatives.

FSE T2WI, DWI and PWI; time to peak (TTP) maps and regional cerebral blood volume (rCBV) maps were performed during the acute and subacute stages. Initial MR images were obtained within 56 hours of onset and follow-up studies were performed during the 2nd week after the ischemic attack. SPECT imaging was performed within 2 hours of MR imaging during the acute and/or the subacute stages (Table 2).

Fast Spin-Echo T2-weighted MR imaging

FSE T2WI were obtained at 4000/100/2 (repetition time, msec/effective echo time, msec/excitation), with a 256 × 256 matrix, a 20 × 20 cm field of view, 5/2 mm slice thickness/gap, 16 kHz bandwidth and a 3 min 12 sec acquisition time for 20 slices on a 1.5 - T clinical MR system (Horizon, General Electric, Milwaukee, WI, USA).

Diffusion-weighted MR imaging

DWI was performed using a single-shot spin-echo echo-planar imaging (EPI) technique with multislice continuous imaging and images free of motion artifacts. The imaging parameters for DWI were 5000/100/1 (repetition time, msec/effective echo time, msec/excitations), with a 128 × 128 matrix, a 24 × 24 cm field of view, 4/1 mm slice

Table 1. Summary of Patient Data

Case No.	Age/Sex	Imaging time (hr/d)	NIHSS (Initial/2nd wk)	Location of Lesions
1	28/M	56/10	13/11	Rt. BG, P
2	50/M	24/8	7/14	Lt. BG, TO
3	66/F	46/8	11/10	Lt. P
4	63/F	45/14	11/6	Lt. BG, T
5	75/M	46/10	14/5	Lt. P
6	56/M	42/13	19/12	Lt. P
7	70/M	16/10	20/16	Rt. BG, T
8	68/M	24/8	13/5	Lt. BG
9	45/M	27/12	21/14	Lt. BG, T
10	65/F	46/10	17/12	Lt. P

hr, hour; d, day; wk, week; Rt., right; Lt., left; BG, basal ganglia; P, parietal; TO, temporooccipital; T, temporal.

Table 2. Imaging Modalities Performed during the Acute and Subacute Stages of Ischemic Stroke in Each of 10 Patients with 13 Lesions

	Acute and Early Subacute				Late Subacute			
	T2WI	PWI	DWI	^{99m}Tc-ECDSPECT	T2WI	PWI	DWI	^{99m}Tc-ECDSPECT
Case 1a	+	+	+	+	+	+	+	+
Case 1b	+	+	+	+	+	+	+	+
Case 2a	+	+	+	+	+	+	+	+
Case 2b	+	+	+	+	+	+	+	+
Case 3	+	+	+	+	+	+	+	+
Case 4	+	+	+	+	+	+	+	+
Case 5a	+	+	+	+	+	+	+	+
Case 5b	+	+	+	+	+	+	+	+
Case 6	+	+	+	+	+	+	+	-
Case 7	+	+	+	+	+	+	+	-
Case 8	+	+	+	-	+	+	+	+
Case 9	+	+	+	-	+	+	+	+
Case 10	+	+	+	-	+	+	+	+
Total	13	13	13	10	13	13	13	11

thickness/gap, 91 kHz bandwidth, 90° flip angle and 50 sec acquisition time for 140 images (10 single-shot EPI in each of 14 slices). The EPI pulse sequence supplied by the manufacturer was modified to acquire the images with multiple values along multiple axes. The b factors used were 0, 333, 666, and 1000 sec/mm^2, which these were applied to the x, y, and z directions, respectively. Stroke was evaluated using a transverse slice orientation. Images with b factors of 1000sec/mm^2 and in the z direction were used to make image comparisons. To enable direct comparisons with PWI, the same slice thickness and gap were used.

Perfusion-weighted MR imaging

PWI were performed using the dynamic first-pass bolus tracking of gadopentetate dimeglumine (Magnevist, Schering, Germany) with an EPI gradient-echo sequence. The gadolinium bolus (0.2 mmol/kg) was administered intravenously using an 18-guage catheter placed in an antecubital vein by manual injection over a period of 5 seconds, followed by a 30 ml saline flush. The manual injection was undertaken by an experienced doctor to ensure it was performed under the same conditions in all patients. Imaging parameters for PWI were 1500/65/1 (repetition time, msec/effective echo time, msec/excitations), using a 256 × 192 matrix, 24 × 24 cm field of view, 4/1 mm slice thickness/gap, 91 kHz bandwidth, 90° flip angle and a 2 min 2 sec acquisition time for 240 images (80 phases of single-shot EPI in each of 3 slices). Three transaxial slices, which showed high signal intensity by DWI, were selected for comparison with T2WI, DWI and ^{99m}Tc-ECD SPECT. Upper slices to the frontal sinus were chosen to avoid magnetic susceptibility artifacts. The dynamic perfusion series were processed on a pixel-by-pixel basis using a customized commercial image analysis software program (IDL; Interactive Data Language, Research System Inc., CO, USA) to produce TTP and rCBV maps (see next paragraph). By applying tracer kinetic principles, a gamma-variate function was fitted to the relaxivity (concentration-time) curve to eliminate recirculation effects in the rCBV map.

The signal-time curve for each pixel was trnsformed to the relaxivity curve (ΔR_2^* curve) using the following equation:

$$\Delta R_2^* = 1/T2^* = -1/TE \ \ln (S(t)/S(0)), \quad (1)$$

where ΔR_2^* is change in transverse relaxation rate and T2* represents dephasing due to magnetic field inhomogeneities. TE is echo time. S(t) is the signal intensity at time t and S(0) is the signal intensity at time 0.

The ΔR_2^* curve was calculated to generate each rCBV map. TTP was defined as the time from the beginning of dynamic change to the ΔR_2^* curve maxima and TTP map was constructed from the TTP value of each pixel.

SPECT imaging

One hour after the intravenous administration of 740MBq (20 mCi) of ^{99m}Tc-ECD, SPECT imaging was performed using a brain-dedicated annular crystal gamma camera (Digital Scintigraphic Inc, Waltham, USA) equipped with low-energy high-resolution parallel-hole collimators. Images were acquired in a 128 × 128 image matrix over 120 projections at 3° angular increments. A minimum of 60,000 counts per view were obtained with an upper limit of 20 sec of acquisition time per view. Transaxial images were reconstructed by the filtered-back projection method using a Butterworth filter (Nyquist frequency 1.1 cycle/cm at an order No. 10). Attenuation correction of the transaxial images was performed using Chang's method. Coronal and sagittal slices were calculated from the original transaxial images. The slice thickness of the transaxial images was 5 mm without any gap. Image planes were adjusted to have the same level and orientation as the MR images.

Data analysis

Qualitative comparison of MR images and ^{99m}Tc-ECD SPECT images. PWI and DWI were compared with ^{99m}Tc-ECD SPECT in terms of lesion detectability and apparent lesion size and in terms of the estimated size of the final infarct lesion during the acute and subacute stages. FSE T2WI taken at 3 months after ischemic attack was used to determine the lesion size of final infarction. This qualitative evaluation was performed by two experienced neuroradiologists.

Semi-quantitative comparison of the rCBV maps and ^{99m}Tc-ECD SPECT images. Regions-of-interest (ROI) were decided by comparing the size of the 8 ischemic lesions of 5 patients in initial and follow-up studies. The ischemic core was defined as black area in the ^{99m}Tc-ECD SPECT. The ischemic periphery was defined as a blue area located between the dark ischemic core and normal brain parenchyma (Fig. 1). Care was taken not to include large vessels or hemorrhagic foci. The asymmetry index was calculated using the following equation:

$$AI = (Ci - Cc) \times 200 / (Ci + Cc), \quad (2)$$

where AI represents asymmetry index. Ci is the mean pixel counts (or signal intensity) of the ipsilateral lesion and Cc is the mean pixel counts (or signal intensity) of the normal contralateral hemisphere.

ΔAI was calculated as the change of AI between an initial study during the acute/early subacute stage and a follow-up study in the late subacute stage upon the ischemic core (ΔAI_{core}) and peri-infarct ischemic lesions (ΔAI_{peri}).

$$\Delta AI_{core} = AI_{core}\text{e in the acute/early subacute stage} - AI_{core} \text{ at a late subacute stage} \quad (3)$$

$$\Delta AI_{peri} = AI_{peri} \text{ in the acute/early subacute stage} - AI_{peri} \text{ at a late subacute stage} \quad (4)$$

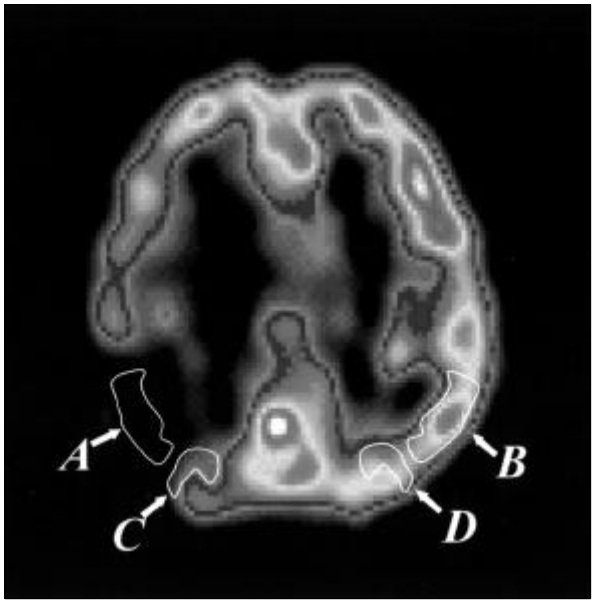

Fig. 1. The asymmetry index (AI) was calculated using the following formula in the ischemic core and in the periphery; AIcore = (CA - CB) × 200 / (CA + CB), AIperi = (CC - CD) × 200 / (CC + CD), where C are the mean pixel counts in the ROIs.

Table 3. Time to Peak (TTP) Values in the Ischemic Core, Periphery and Contralateral Normal Brain Parenchyma during the Acute and Subacute Stages of Ischemic Stroke (sec)

	Acute or Early Subacute			Late Subacute		
	Ischemic lesion		Contralat.	Ischemic lesion		Contralat.
	Core	Periphery	normal	Core	Periphery	normal
Case 1a	*	16.23	12.55	12.23	7.12	6.45
Case 1b	13.12	13.12	12.85	10.15	7.43	6.75
Case 2a	14.26	14.26	7.64	*	15.21	8.33
Case 2b	*	14.34	7.94	12.13	12.13	8.86
Case 3	9.17	9.17	6.56	9.12	9.12	11.02
Case 4	*	14.56	9.15	13.13	13.13	9.25
Case 5a	*	14.21	8.54	*	16.54	11.17
Case 5b	*	14.34	8.54	*	16.54	11.17
Case 6	4.12	4.17	5.34	11.22	11.22	11.15
Case 7	*	11.11	7.21	11.52	11.52	9.96
Case 8	*	14.25	14.23	13.87	13.87	13.11
Case 9	*	16.31	9.13	9.44	9.44	9.13
Case 10	*	9.12	9.13	15.22	9.86	9.26
Mean	*	12.57	9.26	*	11.49	9.77
SD (±)	*	3.56	2.66	*	3.13	1.91

*uncheckable due to severe time delay; Case 2a is not included in the Mean and SD because it is newly developed lesion during the subacute stage.

⊿AI on the rCBV map was compared with that of the corresponding area on the ^{99m}Tc-ECD SPECT images. Data was expressed as mean ± SD. The Wilcoxon Signed-Rank test was used for statistical analysis and a p value of $< .05$ was considered significant.

We were not able to calculate ⊿AI from the TTP maps because of the severe time delays experienced in the ischemic core during the acute stage.

RESULTS

Qualitative comparison of MR images and ^{99m}Tc-ECD SPECT

Acute and early subacute Stage of Ischemic Stroke. In the acute and early subacute stage, the TTP map showed time delays in both the ischemic core and the peri-infarct ischemic lesion. In the contralateral normal region, the TTP was 9.26 ± 2.66 sec (Table 3). Although during the acute stage the TTP map showed a similar area and degree of hypoperfusion in all lesions, the rCBV map showed a similar area and degree of hypoperfusion in only 5/10 lesions. The hypoperfusion areas of the remaining 5 lesions were smaller in the rCBV map than in ^{99m}Tc-ECD SPECT images. On comparing ^{99m}Tc-ECD SPECT with DWI, ^{99m}Tc-ECD SPECT showed larger abnormal areas in all lesions than DWI during the acute stage (Fig. 2 - 4).

Late Subacute Stage of Ischemic Stroke. In the late subacute stage, TTP was improved in the ischemic core in 8/13 lesions. In Case 2a, where the ischemic core had newly developed during the late subacute stage (Fig. 3), TTP was delayed and immeasurable. In the periphery of the subacute stroke, TTP showed either normalized or improved in 12/13 lesions (Table 3).

As compared with ^{99m}Tc-ECD SPECT images in the subacute stage, the TTP map showed similar or smaller areas of hypoperfusion in all lesions. Both DWI and rCBV maps showed smaller abnormal areas than ^{99m}Tc-ECD SPECT in all lesions. In addition, ^{99m}Tc-ECD SPECT showed the infarct core clearly as did the MR images; however, ^{99m}Tc-ECD SPECT better demonstrated the area of decreased perfusion adjacent to the

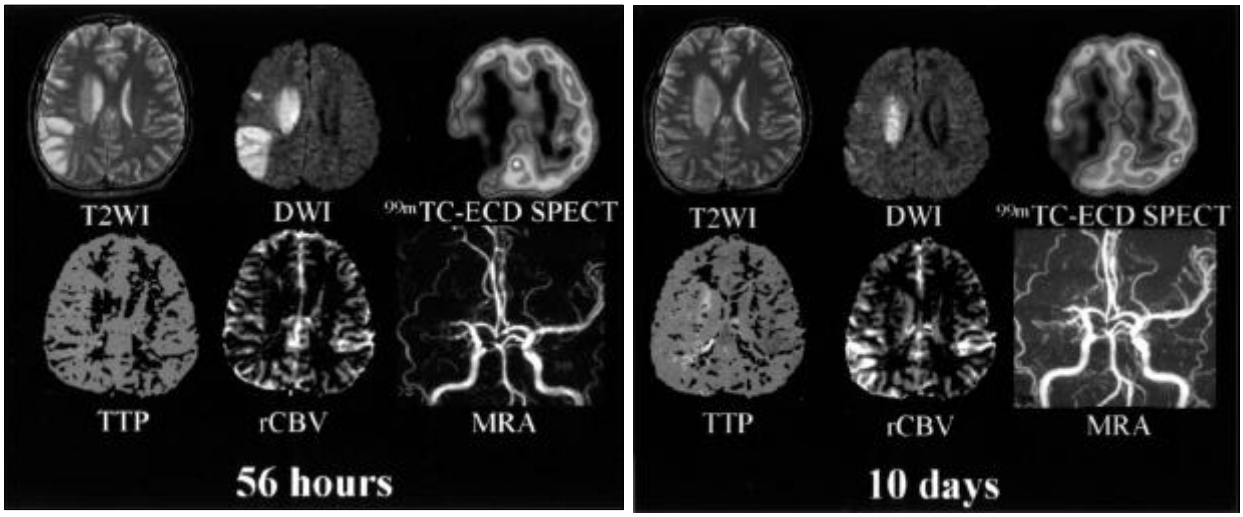

Fig. 2. A 28-year-old man with severe left hemiplegia and dysarthria (Case 1). Fifty-six hours after ischemic attack, TTP map shows a perfusion defect in the right basal ganglia (Case 1a) and a slight time delay in the right parietal area (Case 1b), which is in the same region as the decreased perfusion observed by ^{99m}Tc-ECD SPECT. However, the TTP map is not able to localize the ischemic core in the right parietal lesion. The rCBV map also shows a little asymmetry of cerebral blood volume in the right parietal lesion (asymmetry index: 1.5). T2WI and DWI show discrete high signal intensity in the ischemic core, but they do not show the mildly injured area adjacent to the core. Images taken 10 days after the ischemic attack show normal signal intensity on T2WI and DWI due to pseudonormalization and/or to a slight improvement. Unlike ^{99m}Tc-ECD SPECT, the TTP map does not localize the infarct core in the right parietal lesion. Initial and follow-up MRA show occluded right M1. This patient's condition improved to mild left hemiplegia one month after the ischemic attack (NIHSS 13 →11 →4).

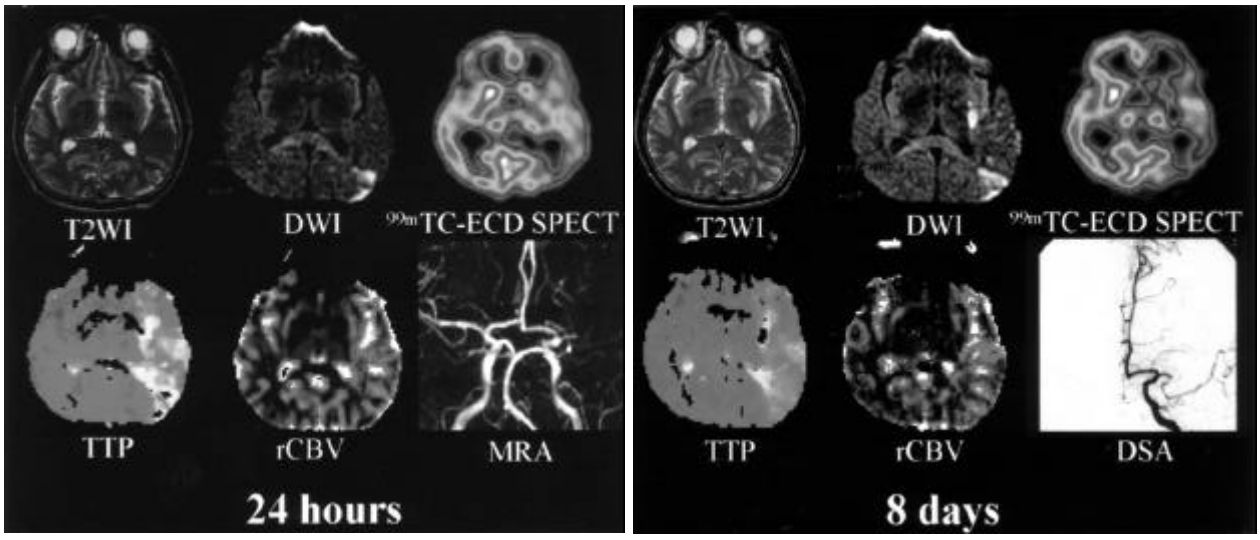

Fig. 3. A 50-year-old man with right hemiplegia and dysarthria (Case 2). Twenty-four hours after ischemic attack, ^{99m}Tc-ECD SPECT shows a diffusely decreased uptake in the left temporal lobe, which was most prominent in the temporooccipital area (Case 2b). This abnormality in ^{99m}Tc-ECD SPECT matches well with the TTP map. T2WI and DWI show a patch of high signal intensity only in the left temporooccipital area of the ischemic core. In images taken 8 days after the ischemic attack, high signal intensity area has developed in the posterolateral aspect of the left basal ganglia (Case 2a) on T2WI and DWI, which matched decreased uptake by ^{99m}Tc-ECD SPECT. The TTP map showed severe time delay in the left basal ganglia. In the left temporooccipital lesion, persistent high signal intensity by T2WI and DWI and a further decreased uptake on ^{99m}Tc-ECD SPECT are observed. Both the TTP and rCBV maps are unable to localize the infarct core of the left temporooccipital lesion due to improved perfusion. Initial MRA and follow-up DSA show occluded left M1.

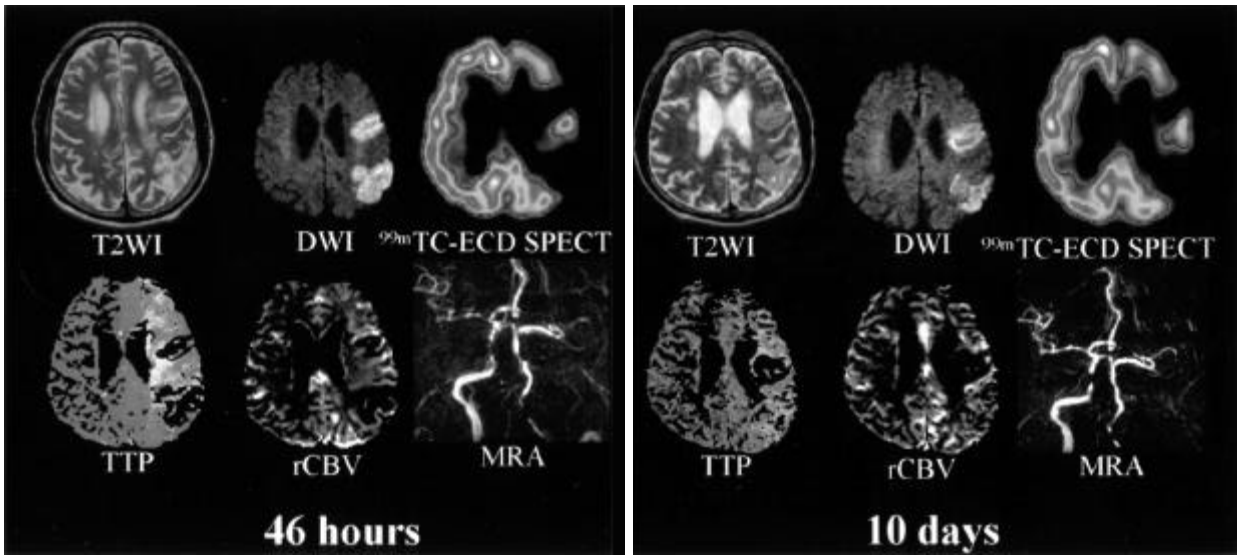

Fig. 4. A 75-year-old man with right hemiplegia and dysarthria (Case 5). Forty-six hours after ischemic attack, ^{99m}Tc-ECD SPECT, TTP and rCBV maps show the same area of perfusion defect in the left parietal lobe. T2WI and DWI show high signal intensity only in the 2 separate infarct cores (anterior lesion: Case 5a, posterior lesion: Case 5b). Images taken 10 days after the ischemic attack show persistent defect by ^{99m}Tc-ECD SPECT, although perfusion improved slightly in the posterior parietal core in the TTP and rCBVmaps. Left ICA is not seen on initial and follow-up MRA.

infarct lesion caused by recent insult than did the MR images (Fig. 2 - 4).

Semi-quantitative comparison of rCBV map and ^{99m}Tc-ECD SPECT

Comparison of ⊿AI on the rCBV Map with the corresponding ⊿AI of ^{99m}Tc-ECD SPECT. In the ischemic core, ⊿AI on the rCBV (-88.44 ± 65.80) map was higher than that on ^{99m}Tc-ECD SPECT (-27.35 ± 14.84), but this was without statistical significance ($p = 0.063$). In the ischemic periphery, ⊿AI on the rCBV (-60.99 ± 55.40) map was higher than that on the ^{99m}Tc-ECD SPECT images (-7.62 ± 5.06), again without statistical significance ($p = 0.091$) (Table 4, 5, Fig. 5). ⊿AI on the TTP map was not included in this comparison due to the severely delayed and immeasurable nature of TTP values in the ischemic core during the acute and early subacute stages.

Comparison of ⊿AI of the Ischemic Core with that of the Ischemic Periphery. In the rCBV map, ⊿AI was not significantly different in the ischemic core and the periphery. However, ^{99m}Tc-ECD SPECT showed a statistically significant difference in ⊿AI between the two ($p = 0.028$). Despite the fact that cerebral perfusion had improved in the periphery during the late subacute stage, by ^{99m}Tc-ECD SPECT, the effect of improved perfusion on cell function was significantly higher in the ischemic core (Table 4 and 5, and Fig. 6).

Detectability of the final infarct lesion

In the acute and early subacute stages, ^{99m}Tc-ECD SPECT identified all of the lesions. However, MR images did not detect 2/10 lesions; specifically, normal signal intensity on T2WI and DWI in the left basal ganglia lesion of case 2a, and an almost normal rCBV coupled with a failure to localize the infarct core in the TTP map of the right parieto-occipital area in case 1b (Table 6, Fig. 2, 3).

In the late subacute stage, ^{99m}Tc-ECD SPECT identified all of the final infarct lesions showing persistent defect or slightly increased uptake compared to the acute and early subacute stage (Figs. 2 - 4). However, MR images did not identify 5 final infarct lesions; Case 1a in the rCBV map, Case 1b in the T2WI, DWI and TTP maps, Case 2b in the rCBV and TTP maps, Case 3 in the rCBV and TTP maps, and Case 9 in the DWI, due to

Table 4. Asymmetry Indices of ^{99m}Tc-ECD SPECT Radioactivity Count in the Ischemic Core and Periphery during the Acute and Subacute Stages of Ischemic Stroke

	AI_{core}		AI_{peri}		ΔAI_{core}	ΔAI_{peri}
	A or ES	LS	A or ES	LS		
Case 1a	-117.06	-90.90	-62.62	-50.43	-26.16	-12.19
Case 1b	-110.52	-61.53	-48.42	-45.04	-48.99	-3.38
Case 2a	-32.83	-78.99	-29.41	-59.37	46.16	29.96
Case 2b	-60.46	-56.84	-38.29	-34.61	-3.62	-3.68
Case 3	-83.15	-44.21	-47.06	-32.00	-38.94	-15.06
Case 4	-100.00	-80.60	-22.68	-20.31	-19.40	-2.37
Case 5a	-161.32	-127.40	-58.99	-47.86	-33.92	-11.13
Case 5b	-130.81	-110.42	-57.54	-52.00	-20.39	-5.54
Mean	-109.04	-81.70	-47.94	-40.32	-27.35	-7.62
SD (±)	32.62	30.08	13.91	11.69	14.84	5.06

AI_{core}, asymmetry index in the ischemic core;
AI_{peri}, asymmetry index in the ischemic periphery;
A, acute; ES,early subacute; LS, late subacute;
ΔAI_{core}, AI_{core} in acute or early subacute stage - AI_{core} in late subacute stage;
ΔAI_{peri}, AI_{peri} in acute or early subacute stage - AI_{peri} in late subacute stage;
Case 2a is not included in the Mean and SD because it is newly developed lesion during the subacute stage.

Table 5. Asymmetry Indices of Rcbv in the Ischemic Core and Periphery during the Acute and Subacute Stages of Ischemic Stroke

	AI_{core}		AI_{peri}		ΔAI_{core}	ΔAI_{peri}
	A or ES	LS	A or ES	LS		
Case 1a	4.01	5.10	46.77	5.10	-1.09	41.67
Case 1b	1.50	93.28	1.50	93.28	-91.78	-91.78
Case 2a	-34.03	-115.23	-37.05	-27.45	81.20	-9.60
Case 2b	-108.60	28.57	-50.68	28.57	-137.18	-79.25
Case 3	-71.41	7.94	-15.03	45.51	-79.35	-60.54
Case 4	-173.96	-20.40	-150.44	-10.23	-153.57	-140.21
Case 5a	-200.00	-197.52	-35.57	14.47	-2.48	-50.04
Case 5b	-200.00	-46.34	-35.57	11.21	-153.66	-46.78
Mean	-106.92	-18.48	-34.14	26.84	-88.44	-60.99
SD (±)	88.64	90.17	60.53	34.18	65.80	55.40

AI_{core}, asymmetry index in the ischemic core;
AI_{peri}, asymmetry index in the ischemic periphery;
A, acute; ES, early subacute; LS, late subacute;
ΔAI_{core}, AI_{core} in acute or early subacute stage - AI_{core} in late subacute stage;
ΔAI_{peri}, | AI_{peri} in acute or early subacute stage - AI_{peri} in late subacute stage;
Case 2a is not included in the Mean and SD because it is newly developed lesion during the subacute stage.

either improved perfusion or pseudonormalization (Table 6, Fig. 2, 3). FSE T2WI taken at 3 months after ischemic attack disclosed an encephalomalatic cavity in all lesions of high signal intensity in the initial or follow-up T2WI and DWI.

DISCUSSION

Perfusion-weighted MR imaging is used to track the changes, which occur during the first-pass transit of injected contrast bolus agent through the brain. After ischemia, perfusion defi-

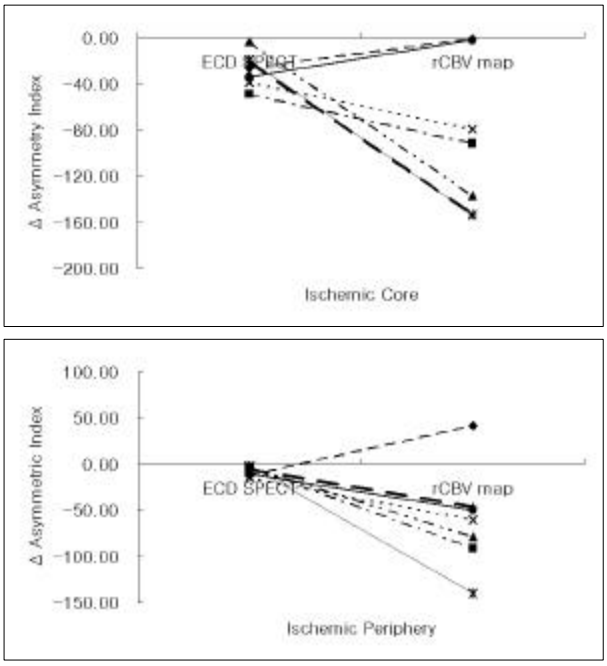

Fig. 5. Comparison between ΔAI by ^{99m}Tc-ECD SPECT and rCBV map (Wilcoxon Signed-Rank test).

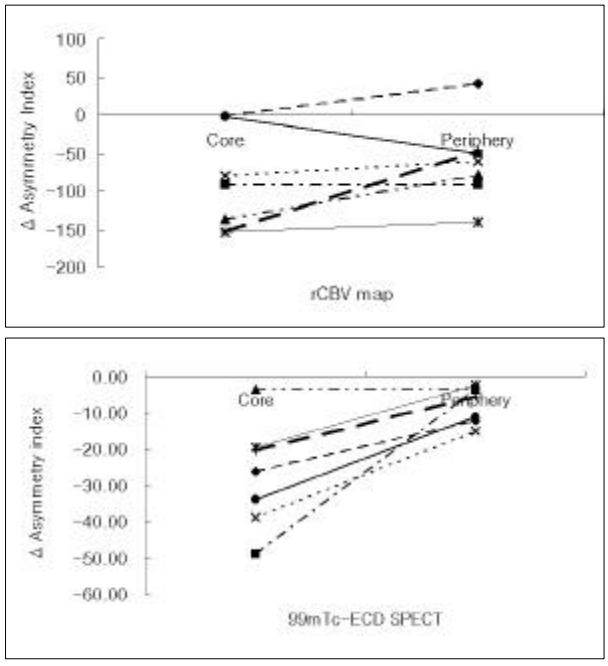

Fig. 6. Comparison between ΔAI of the ischemic core and of the ischemic periphery (Wilcoxon Signed-Rank test).

Table 6. Detectability of the Final Infarct Lesion in MR Images and by ^{99m}Tc-ECD SPECT during the Acute and Subacute Stages of Ischemic Stroke (n=10 lesions in acute and early subacute stage, n=11 lesions in late subacute stage)

		MR images				^{99m}Tc-ECD SPECT
		T2WI	TTP	rCBV	DWI	
Identification of Final Infarct Lesion	Acute and Early Subacute	9	9	9	9	10
	Late Subacute	10	8	8	9	11

cit can be observed as a decrease in the concentration of contrast bolus transit. Moreover, the change in the transverse relaxation rate (ΔR_2^*), as measured by perfusion-weighted MR imaging, is linearly related to the concentration of paramagnetic contrast agent remaining in the tissue.[14-16] This bolus tracking method provides a reasonably accurate measure of relative cerebral perfusion changes.

We define two perfusion parameters; the TTP map and the rCBV map. The TTP is the time taken from the beginning of cerebral perfusion to the peak value in the ΔR_2^* curve. Although, MTT should be used for the cerebral blood transit time in the absolute quantification analysis,[17] MTT may be substituted by TTP in a relative quantification. The TTP map shows the area of delayed perfusion and gives a distinct boundary between the areas of normal and abnormal perfusion. During the acute stage of ischemic stroke, the lesion size appeared larger in the TTP map than in the rCBV map, DWI or T2WI. This is because the abnormal area in the TTP map is comprised of the infarct core and the peri-infarct ischemia, which is similar to the anomalous perfusion area observed by ^{99m}Tc-ECD SPECT. However, some differences exist between the ^{99m}Tc-ECD SPECT images and the TTP map; for although ^{99m}Tc-ECD SPECT can localize the infarct core and the peri-infarct ischemia in the same vascular territory, the TTP map can not in some cases. This is particularly true of the infarct core during the subacute stage. With the aid of the TTP map, one can identify areas prone to future ischemic injury as exemplified by

the basal ganglia lesion of the present study (Fig. 3). At the time of the initial examination, the basal ganglia lesion may have been in the very early hyperacute stage, which even DWI can not detect. Only the TTP map and the ^{99m}Tc-ECD SPECT images showed an abnormality in this region. This suggests that if PWI was unavailable, ^{99m}Tc-ECD SPECT could play the role of PWI during the acute stage of an ischemic stroke.

The rCBV map is obtained by integrating the ΔR_2^* curve during the first passage of contrast agent and represents the regional cerebral blood volume. The abnormal portion of the rCBV map was found to be smaller than that found either by TTP map or by ^{99m}Tc-ECD SPECT, because the rCBV map showed only the acute stroke lesion which represents the final infarction and moreover, the rCBV map does not show peri-infarct ischemia.[10] ΔAI by rCBV map was larger than Δ AI determined by ^{99m}Tc-ECD SPECT in both the ischemic core and the periphery. This means that the rCBV map is hemodynamically more sensitive than ^{99m}Tc-ECD SPECT because the rCBV map does not express the tissue viability state, but this feature is a disadvantage of rCBV map in the evaluation of ischemic stroke.

Diffusion-weighted MR imaging applies diffusion-sensitized gradients which make the collected MR signal sensitive to the incoherent motions of water protons.[18] After ischemia, acute cell swelling and changes in cell membrane permeability result in reduced water diffusion, thus increasing the DWI signal intensity.[19,20] DWI can detect acute ischemic stroke within 1hour of MCA occlusion in the experimental models.[18,21] PWI accompanied by DWI can identify tissue at risk, which is achieved by identifying regions of mismatched PWI and DWI.[8,9,22,23] Intra-arterial thrombolysis candidates can be identified during the hyperacute stage when they have either a PWI/DWI mismatch or a decreased DWI apparent diffusion coefficient (ACD).

However, in the subacute stage, conventional MRI and DWI show a "fogging effect" or "pseudonormalization" due to decreased edema and the temporal normalization of the ACD value.[24,25] PWI also shows improved flow "luxury perfusion" in the areas of acutely compromised perfusion.[26] This behavior makes it difficult to evaluate ischemic lesions. However, ^{99m}Tc-ECD SPECT is insensitive to luxury perfusion during the subacute stage.[3-5] ^{99m}Tc-ECD is a radiochemically stable brain perfusion agent and shows good image contrast and spatial resolution.[3,27,28] After rapid uptake of lipophilic ^{99m}Tc-ECD by the normal brain, it is retained within the brain by a rapid de-esterification to a polar metabolite which does not re-cross the blood-brain barrier.[28-30]

During the examination of the acute and early subacute stage in the present study, ^{99m}Tc-ECD uptake in the ischemic periphery was less severely reduced than in the ischemic core, because cells in the ischemic periphery had a relatively preserved function. In the late subacute stage of ischemic stroke, cells in the ischemic core which were viable, though dysfunctioning recovered their enzymatic activity after reperfusion and ^{99m}Tc-ECD uptake correspondingly increased. However, in the ischemic periphery, mild or moderate enzyme activity dysfunction during the acute stage recovered to a lesser extent. Consequently, ΔAI was significantly higher in the ischemic core than in the ischemic periphery by ^{99m}Tc-ECD SPECT. This result demonstrates that ^{99m}Tc-ECD is useful for assessing both brain tissue viability and enzymatic activity. This result is consistent with previous reports that ^{99m}Tc-ECD uptake in the infarct lesion is very low in despite of luxury perfusion during the subacute stage of ischemic stroke and suggests that ^{99m}Tc-ECD might be useful to assess brain tissue viability.[3-5,27,28] Improvement in the neurologic dysfunction of patients supports this result. The ability of ^{99m}Tc-ECD SPECT to directly depict tissue damage is superior to that of MR images during the subacute stage of an ischemic stroke. Pseudonormalization in T2WI and DWI and luxury perfusion in PWI inhibit the proper evaluation of tissue viability by MR images.

Although initial imaging is performed during the acute stage of ischemic stroke, a new lesion of the hyperacute stage or an evolving stroke may be present. TTP map and ^{99m}Tc-ECD SPECT allow assessment of the vulnerability of this region. In the acute stage of ischemic stroke, ^{99m}Tc-ECD SPECT and PWI findings are substantially in agreement. Although, T2WI, DWI or PWI may miss both newly developing and improved perfusion lesions, ^{99m}Tc-ECD SPECT was found to be able to

detect all acute ischemic lesions. During the subacute stage of ischemic stroke, ^{99m}Tc-ECD SPECT was able to detect all lesions without the pseudonormalization seen in MR images. In addition, it was always able to localize the infarct core and peri-infarct ischemia in all lesions examined in both the acute and subacute stages. Moreover, ^{99m}Tc-ECD SPECT is a valuable tool for the evaluation of cell viability and function. This can undoubtedly be widely applied to other situations, which require the evaluation of cell viability and enzymatic activity.

In summary, ^{99m}Tc-ECD SPECT is comparable to PWI in terms of its ability to detect acute stroke and may be more useful than PWI in the case of subacute infarction.

REFERENCES

1. Steinling M, Huglo D, Kolesnikov H, Vergnes R, Rousseaux M. 'Normal' ^{99m}Tc-HmPAO Distribution in Large Subacute Middle Cerebral Artery Infarct. Stroke 1994;25:2507-8.
2. Cheeseman EH, Blanchette MA, Ganey MV, Maheu LJ, Miller SJ, Watson AD. Technetium-99m-ECD: ester derivertized diaminedithiol Tc complexes for imaging brain perfusion [abstract]. J Nucl Med 1988;29:788.
3. Lassen NA, Sperling B. ^{99m}Tc-Bicisate reliably images CBF in chronic brain diseases but fails to show reflow hyperemia in subacute stroke: report of multicenter trial of 105 cases comparing 133Xe and ^{99m}Tc-Bicisate (ECD, Neurolite) measured by SPECT on same day. J Cereb Blood Flow Metab 1994;14 Suppl:S44-8.
4. Nakagawara J, Nakamura J, Takeda R, Okumura T, Seki T, Hayase K, et al. Assessment of postischemic reperfusion and diamox activation test in stroke using ^{99m}Tc-ECD SPECT. J Cereb Blood Flow Metab 1994;14 Suppl:S49-57.
5. Shishido F, Uemura K, Murakami M, Inugami A, Ogawa T, Fujita H, et al. Cerebral uptake of Tc-99m-ECD in patients with cerebrovascular disease in comparison with CBF and CMRO2 measured by positron emission tomography. J Cereb Blood Flow Metab 1994; 14 Suppl:S66-S75.
6. Bryan RN, Levy LM, Whitlow WD, Killian JM, Preziosi TJ, Rosario JA. Diagnosis of acute cerebral infarction: comparison of CT and MR imaging. Am J Neuroradiol 1991;12:611-20.
7. Yuh WT, Crain MR, Loes DJ, Greene GM, Ryals TJ, Sato Y. MR imaging of cerebral ischemia: findings in the first 24 hours. Am J Neuroradiol 1991;12:621-9.
8. Baird AE, Benfield A, Schlaug G, Siewert B, Lovblad KO, Edelman RR, et al. Enlargement of human cerebral ischemia lesion volumes measured by diffusion-weighted magnetic resonance imaging. Ann Neurol 1997;41:581-9.
9. Warach S, Wielopolski P, Edelman RR. Identification and characterization of the ischemic penumbra of acute human stroke using echo planar diffusion and perfusion imaging. In: Proc Twelfth Ann Sci Mtg Soc Magn Res Med 1993;263.
10. Rordorf G, Koroshetz WJ, Copen WA, Cramer SC, Schaefer PW, Budzik RF, et al. Regional ischemia and ischemic injury in patients with acute middle cerebral artery stroke as defined by early diffusion-weighted and perfusion-weighted MRI. Stroke 1998;29:939-43.
11. Rother J, DeCrepigny AJ, D'Arceuil H, Moseley ME. MR detection of cortical spreading depression immediately after focal ischemia in the rat. J Cereb Blood Flow Metab 1996;16:214-20.
12. Sorensen AG, Buonanno FS, Gonzalez RG, Schwamm LH, Lev MH, Huang-Hellinger FR, et al. Hyperacute stroke: evaluation with combined multisection diffusion-weighted and hemodynamically weighted echo-planar MR imaging. Radiology 1996;199:391-401.
13. Gordon DL, Bendixen BH, Adams HP, Clarke W, Kappelle LJ, Woolson RF. Interphysician agreement in the diagnosis of subtypes of acute ischemic stroke: implications for clinical trials. The TOAST investigators. Neurology 1993;43:1021-7.
14. Belliveau JW, Rosen BR, Kantor HL, Rzedzian RR, Kennedy DN, McKinstry RC, et al. Functional imaging by susceptibility-contrast NMR. Magn Reson Med 1990;14:538-46.
15. Weisskoff RM, Chesler D, Boxerman JL, Rosen BR. Pitfalls in MR measurement of tissue blood flow with intravascular tracers: which mean transit time? Magn Reson Med 1993;29:553-9.
16. Maeda M, Itoh S, Ide H, Matsuda T, Kobayashi H, Kubota T, et al. Acute stroke in cats: Comparison of dynamic susceptibility-contrast MR imaging with T2- and diffusion-weighted MR imaging. Radiology 1993; 189:227-32.
17. Ostergaard L, Sorensen AG, Kwong KK, Weisskoff RM, Gyldensted C, Rosen BR. High Resolution Mesurement of Cerebral Blood Flow using Intravascular Tracer Bolus Passages. Part II: Experimental Comparison and Preliminary Results. Magn Reson Med 1996;36:726-36.
18. Le Bihan D, Breton E, Lallemand D, Aubin M, Vignaud J, Laval-Jeantet M. Separation of diffusion and perfusion in intravoxel incoherent motion MR imaging. Radiology 1988;168:497-505.
19. Moseley ME, Cohen Y, Mintorovitch J, Chileuitt L, Shimizu H, Kucharczyk J, et al. Early detection of regional cerebral ischemia in cats: comparison of diffusion- and T2-weighted MRI and spectroscopy. Magn Reson Med 1990;14:330-46.
20. Minematsu K, Li L, Fisher M, Sotak CH, Davis MA, Fiandaca MS. Diffusion-weighted MRI: rapid and quantitative detection of focal brain ischemia. Neurology 1992;42:235-40.

21. Kim HS, Kim DI, Jeong EK, Shin YS, Yoon PH, Hwang YJ, et al. MR imaging of experimental focal cerebral ischemia in cats: temporal evolution of hyperacute stroke. J Korean Radiol Soc 1999;41:453-9.
22. Baird AE, Warach S. Magnetic Resonance Imaging of Acute Stroke. J Cereb Blood Flow Metab 1998;18:583-60.
23. Warach S, Dashe JF, Edelman RR. Clinical outcome in ischemic stroke predicted by early diffusion-weighted and perfusion magnetic resonance imaging: a preliminary analysis. J Cereb Blood Flow Metab 1996;16:53-9.
24. Warach S, Chien D, Li W, Ronthal M. Fast magnetic resonance diffusion-weighted imaging of acute human stroke. Neurology 1992;42:1717-23.
25. Warach S, Gaa J, Siewert B, Wielopolski P, Edelman R. Acute human stroke studied by whole brain echo planar diffusion weighted MRI. Ann Neurol 1995;37:231-41.
26. Lassen NA. The luxury perfusion syndrome and its possible relation to acute metabolic acidosis localised within the brain. Lancet 1966;2:113-5.
27. Holman BL, Hellman RS, Goldsmith SJ, Mena IG, Leveille J, Gherardi PG, et al. Biodistribution, dosimetry and clinical evaluation of technetium-99m ethyl cysteinate dimer in normal subjects and in patients with chronic cerebral infarction. J Nucl Med 1989;30: 1018-24.
28. Tsuchida T, Nishizawa S, Yonekura Y, Sadato N, Iwasaki Y, Fujita T, et al. SPECT images of technetium-99m-ethyl cysteinate dimer in cerbrovascular disease: comparison with other cerebral perfusion tracers and PET. J Nucl Med 1994;35:27-31.
29. Walovitch RC, Franceschi M, Picard M, Cheesman EH, Hall KM, Makuch J, et al. Metabolism of ^{99m}Tc-L,L-ethyl cysteinate dimer in healthy volunteers. Neuropharmacology 1991;30:283-92.
30. Walovitch RC, Cheesman EH, Maheu LJ, Hall KM. Studies of the retention mechanism of the brain perfusion imaging agent ^{99m}Tc-Bicisate (^{99m}Tc-ECD). J Cereb Blood Flow Metab 1994;14 Suppl:S4-S11.